

UCSF

UC San Francisco Previously Published Works

Title

Therapeutic deep brain stimulation reduces cortical phase-amplitude coupling in Parkinson's disease.

Permalink

<https://escholarship.org/uc/item/0q64c9c3>

Journal

Nature neuroscience, 18(5)

ISSN

1097-6256

Authors

de Hemptinne, Coralie
Swann, Nicole C
Ostrem, Jill L
[et al.](#)

Publication Date

2015-05-01

DOI

10.1038/nn.3997

Peer reviewed



Published in final edited form as:

Nat Neurosci. 2015 May ; 18(5): 779–786. doi:10.1038/nn.3997.

Therapeutic deep brain stimulation reduces cortical phase-amplitude coupling in Parkinson's disease

Coralie de Hemptinne¹, Nicole Swann¹, Jill L. Ostrem², Elena S. Ryapolova-Webb¹, Marta San Luciano², Nicholas Galifianakis², and Philip A. Starr^{1,3}

¹Department of Neurological Surgery, University of California, San Francisco, 505 Parnassus Avenue, San Francisco, CA, 94143

²Department of Neurology, UCSF, 1635 Divisadero Street, San Francisco, CA, 94143

³UCSF Graduate Program in Neuroscience

Abstract

Deep brain stimulation (DBS) is increasingly applied to the treatment of brain disorders, but its mechanism of action remains unknown. Here, we evaluate the effect of basal ganglia DBS on cortical function using invasive cortical recordings in Parkinson's disease (PD) patients undergoing DBS implantation surgery. In the primary motor cortex of PD patients neuronal population spiking is excessively synchronized to the phase of network oscillations. This manifests in brain surface recordings as exaggerated coupling between the phase of the β rhythm and the amplitude of broadband activity. We show that acute therapeutic DBS reversibly reduces phase-amplitude interactions over a similar time course as reduction in parkinsonian motor signs. We propose that DBS of the basal ganglia improves cortical function by alleviating excessive β phase locking of motor cortex neurons.

Keywords

Parkinson's disease; deep brain stimulation (DBS); electrocorticography (ECoG); primary motor cortex; phase-amplitude coupling

Deep brain stimulation (DBS) is increasingly utilized for therapy of brain disorders, but its mechanism of action remains unclear. This has slowed the development of more effective and less energy intensive stimulation paradigms. The most common clinical application is DBS of the subthalamic nucleus (STN) for Parkinson's disease¹. Most physiological studies of DBS mechanisms in Parkinson's disease have focused on subcortical nuclei, and have suggested that DBS reduces basal ganglia oscillatory activity in the β band (13-30 Hz)²⁻⁸.

Users may view, print, copy, and download text and data-mine the content in such documents, for the purposes of academic research, subject always to the full Conditions of use:http://www.nature.com/authors/editorial_policies/license.html#terms

Corresponding author: Coralie de Hemptinne, Department of Neurological Surgery, University of California, San Francisco, 513 Parnassus Avenue box 0112, San Francisco, CA, 94143. Coralie.dehemptinne@ucsf.edu.

Author Contributions: Conceived and designed the experiments: CDH, PAS. Performed the experiments: CDH, NS, ESR, PAS. Analyzed the data: CDH. Consented patients: CDH, NS, ESR. Recruited patients and characterized patients symptoms: JLO, MSL, NG. Wrote the paper: CDH, PAS. Performed surgical procedures and supervised the project: PAS.

However, the role of β oscillations at the cortical level and the effects of medical or surgical treatments on the amplitude of this brain rhythm are still controversial, as some studies show a decrease in cortical β power associated with successful therapy in PD⁹⁸, while others show an increase¹⁰. Further, comparisons of cortical oscillatory activity between PD and subject without PD have not revealed a difference in the amplitude of β oscillations¹¹⁻¹³. Understanding the mechanisms by which DBS modifies cortical function could lead to an improvement of current therapies

Normal cortical function is dependent on the coupling between the phase of low frequency rhythms and the amplitude of broadband activity (also referred to as broadband γ , 50-200Hz), thought to be a surrogate measure of population spiking¹⁴ and synaptic inputs¹⁵. Phase-amplitude coupling (PAC) has been proposed as a mechanism for communication within and between distinct regions of the brain by coordinating the timing of neuronal activity in brain networks¹⁶. It has been hypothesized that brain rhythms modulate the excitability of neuronal ensembles through fluctuations in membrane potentials, biasing the probability of neuronal spiking at a specific phase of that slower rhythm^{16, 17}. PAC is thought to dynamically link functionally related cortical areas that are essential for task performance¹⁸⁻²¹. In motor cortex, reduction in PAC is a critical step in movement execution^{22, 23}. We recently showed that Parkinson's disease is associated with exaggerated coupling between the phase of β oscillations and the amplitude of broadband activity in the primary motor cortex, likely constraining cortical neuronal activity in an inflexible pattern whose consequence is bradykinesia and rigidity¹³. We hypothesized that DBS exerts its therapeutic effect by normalizing cortical PAC, releasing neuronal pools to engage in task-related activity. To test this, we recorded electrocorticography (ECoG) signals from the motor cortex of Parkinson's disease patients undergoing DBS implantation surgery, before, during and after STN stimulation. Given the role of the basal ganglia–thalamocortical circuit in movement preparation²⁴⁻²⁶ and the facilitation of motor preparation observed during STN DBS²⁷, we also investigated the effect of DBS on movement preparation, movement execution, and alert rest conditions. We showed that therapeutic stimulation decouples high frequency activity from low frequency rhythms in the motor system, both at rest and during a motor task, reversing a fundamental network abnormality of PD.

Results

ECoG potentials were recorded in a total of twenty-three Parkinson's disease patients before, during and after STN stimulation at rest. An example of the cortical and STN electrode locations, as well as the relationship of STN lead location to STN borders determined by microelectrode recordings, are provided in Fig 1 a-c. Twelve of the twenty-three were also tested while performing the arm movement task (Fig 1d-e). Clinical characteristics are provided in Table 1. Representative examples of resting state ECoG potentials recorded from the primary motor cortex (M1) of a Parkinson's disease patient (PD-5) before, during and after STN stimulation, and their respective log power spectral densities are shown in Fig 2. The stimulation artifact was small relative to the cortical signal. As expected, a peak in the β band (13-30Hz) was found in the power spectral densities of M1 ECoG potential, STN LFP, and M1-STN coherence (Fig. 2, Supplementary Fig. 1a and b).

DBS reduces resting state PAC and rigidity

Fig. 3a shows PAC before, during and after STN stimulation for a representative patient (PD-13). A strong interaction was observed between the phase of β oscillations and the amplitude of activity over a broad spectral range of 50-200 Hz, often referred to as “broadband activity” or “broadband γ ” (*left panel*). A similar pattern of PAC was observed in each Parkinson’s disease patient before stimulation. PAC was strongly reduced during STN stimulation (*middle panel*) and increased after the stimulation was turned off (*right panel*). In order to quantify the effect of DBS on this interaction, the modulation index computed for each patient in each condition of stimulation, was averaged across the whole β band and broadband activity (frequency for phase 13-30 Hz; frequency for amplitude 50-200 Hz) as shown by the white dotted box Fig. 3a (*left panel*). This average coupling (*PAC mean*) was computed for each patient, in each condition of stimulation and used for statistical group comparison, using nonparametric tests given its non-normal distribution ($p < 0.001$ Kolmogorov-Smirnov test). Group analysis showed a reduction of PAC during DBS (Fig. 3b, *left panel*). PAC was not back to baseline within five min after DBS when including all patients (Fig. 3b, *right panel*; ranksign test, $p = 0.09$). However, a return to baseline PAC becomes significant when only patients with a DBS induced improvement in symptoms by intraoperative UPDRS scores were selected ($p = 0.014$, $n = 10$). Boxplots of PAC computed in each condition of stimulation including all patients are shown of Fig. 3c (Friedman test, $p = 0.003$). The DBS induced reduction in resting state PAC was insensitive to changes in analysis methods, including eliminating filtering of the stimulus artifact (Supplementary Fig. 2 a-d) and using two alternative methods of calculating the phase amplitude interactions (phase-locking value and cross-frequency coherence, Supplementary Fig. 2 e). The effect was also specific to the primary motor cortex (Supplementary Fig. 1c) and changes in PAC occurred 2-4 s after DBS was turned on or off (Supplementary Fig. 3). These results suggest that the reduction of PAC by acute DBS is not due to the presence of stimulation artifact.

Acute DBS also reduced parkinsonian motor signs as reflected in the rigidity score measured intraoperatively (UPDRS item 22, Fig. 3d, Friedman test $p = 0.0004$). A significant correlation between *PAC mean* and the intraoperative rigidity score was observed before DBS (spearman correlation, $p = 0.014$; $r = 0.54$) and after DBS (spearman correlation; $p = 0.04$; $r = 0.46$) but not with the tremor score. However, we did not find a significant correlation between rigidity reduction and DBS induced change in PAC, likely due to the low range of rigidity changes (rigidity changes = 0-2). To address the problem of the bias inherent in unblinded assessment of motor signs, we tested different stimulation settings (therapeutic and non-therapeutic) in a randomized paradigm, with motor evaluation by a blinded neurologist. This showed a clear relationship between the magnitude of PAC and symptoms severity (Supplementary Fig. 4). In addition, to establish that acute intraoperative stimulation occurred at settings that were relevant to chronic therapeutic DBS, stimulation parameters used intra-operatively were compared to those used for long term therapy, and found to be similar in contact choice, intensity, and frequency (Supplementary Table 1).

Medication has been shown to modulate the frequency at which PAC occurred in the STN of PD^{28, 29}. Therefore, in order to better characterize the effect of DBS on PAC, we also

determined the preferred phase of the coupling (*PAC preferred phase*), the frequencies involved in maximal coupling (*PAC phase freq* and *PAC amp freq*). None of these variables were affected by DBS (Friedman test, $p>0.05$, Supplementary Table 2) suggesting that DBS reduces the magnitude of PAC without changing the preferred phase or frequencies involved in such coupling.

The DBS effect on PAC at rest is not due solely to changes in M1 β or broadband power

A significant correlation between PAC and β power across subjects was observed in all condition of stimulation (before $p=0.0062$, $r=0.56$; during $p=0.0008$, $r=0.66$; after DBS $p=0.0057$, $r=0.56$). This correlation is expected based on the analysis method: greater β power would lead to a more precise estimate of β phase in the calculation of PAC. To verify that this was not the only reason for the PAC change, we performed additional analyses to examine the effects of DBS on β and broadband activity, to see whether the DBS effect on PAC is strongly related to DBS effects on spectral power in these frequency bands. Several parameters were extracted from the M1 ECoG power spectrum in order to better characterize the β band spectral peak and its modulation by DBS. We found the frequency of the β peak (*β peak freq*), its power (*β peak*) and its average over the β band (13-30 Hz, *log β*) were similar irrespective of the stimulation condition (Fig. 4a, Friedman test, $p>0.05$, Supplementary Table 2). This was true even when dividing β power into low β (13-20Hz) and high β (20-30Hz bands, Supplementary Fig. 5). Broadband activity, thought to reflect a combination of spiking and synaptic activity, is not characterized by a peak in the power spectral density. As shown on Fig. 4b, the average log PSD over the broadband was not affected by DBS (*log broadband*). A significant decrease of PAC during DBS was found in patients with a decrease in β power (13 patients) as well as in those with an increase β power (10 patients, Supplementary Fig. 6) suggesting that although both, PAC and β power are correlated, the DBS-induced reduction in PAC is not related solely to a reduction in cortical β power. Of note, as has been reported previously^{3, 5, 8, 30}, we did find that acute DBS reduced STN β power in most cases (Supplementary Fig. 1b), so the effect of DBS on β power differs between cortex and STN.

Movement and DBS reduce PAC during task performance

Given that therapeutic intervention could have different effects on different aspects of movement²⁷, cortical synchronization was also studied while patients performed a reaching movement task allowing us to distinguish three phases; the 'hold' phase during which the patient resting the hand on a button while looking at a fixation point on the screen, the 'preparation' phase during which a target appeared on the screen, and a 'movement' phase during which patient touching the target on screen (Fig. 1c). Examples of ECoG potentials recorded in M1 of PD-1 and the corresponding accelerometry traces are showed on Fig. 5a. The effect of task phases and stimulation conditions on PAC in an individual patient is shown on Fig. 5b (PD7). PAC was reduced from hold (*left panel*) to preparation phase (*middle panel*) and was even further reduced during movement execution (*right panel*). In all three phases, STN DBS induced an additional reduction of PAC (*middle row*) that partly returned to baseline after stimulation was stopped (*lower row*). A significant reduction of PAC by task phases was found in group analyses (Supplementary Table 3. and Fig. 6; Friedman test $p<0.001$). STN DBS significantly reduced this coupling in all three phases

(Friedman test $p < 0.001$) and after DBS, PAC increased toward values observed before STN stimulation (Friedman test $p < 0.001$). A reduction of movement duration (time from movement initiation to movement stop) was observed during DBS (mean \pm std of movement duration in seconds; before DBS 6.1 ± 2.0 ; during DBS 5.4 ± 1.6 ; after DBS 5.8 ± 2.0) showing a reversible therapeutic effect of DBS on bradykinesia during task performance. We did not find a DBS induced improvement in reaction time during the task (Friedman test, $p > 0.05$). This may relate to the patients fatigue or the task paradigm: to avoid anticipatory responses, patients were instructed to move only after the occurrence of the go signal and not to move as fast as possible after its occurrence.

The DBS effect on PAC during a movement task is not due solely to changes in β or broadband power

A strong decrease in the β band during both movement preparation and movement execution was observed (Fig. 7a and b) as has been well documented in persons without movement disorders^{23, 31}. Movement related β changes were not significantly affected by the condition of stimulation (Supplementary Table 4; *β changes*; Friedman test; $p > 0.05$). Another normal feature of movement related change in the sensorimotor cortex is an increase in broadband power that is thought to reflect local cortical activation^{23, 32}. Here, we found a significant increase in broadband power at movement onset that was similar in all three stimulation conditions (Fig. 7a and c; Supplementary Table 5; *broadband power changes*; Friedman test; $p > 0.05$). These results show that similar to the resting state DBS during a movement task does not consistently modulate β or broadband activity but decreases the interaction between both frequency bands.

Discussion

To understand the mechanism of therapeutic brain stimulation, we investigated the effect of STN DBS on primary motor cortex in Parkinson's disease patients undergoing physiologically guided DBS electrode placement in the awake state. We found that interactions between the phase of the β rhythm and the amplitude of broadband activity were decreased during acute therapeutic DBS both at rest and during all elements of a movement task (hold, preparation, and movement). Although the magnitude of β phase-broadband amplitude PAC is correlated to the amplitude of the β oscillation, only the former was consistently affected by DBS. Our results underscore the importance of exaggerated PAC in Parkinson's disease¹³, point to a novel mechanism for the therapeutic effect of DBS, and suggest the incorporation of cortical PAC measures into the design of closed-loop DBS paradigms.

Attenuation of PAC

PAC is thought to be an important mechanism for the coordination between anatomically dispersed neuronal cell assemblies, both in motor function^{22, 23} and in cognitive functions such as memory, learning and attention^{16, 19, 21, 23, 33-35}. Recently, we showed that β -broadband activity coupling is excessive in the arm motor cortex of Parkinson's disease¹³, compared to other movement disorders not involving the arm, and to humans without a movement disorder. Although the origin of excessive PAC is still unclear, recent works

suggest that this feature of PD might arise from an inability of the dopamine-denervated striatum to adequately filter and attenuate β oscillations originating from the cortex¹³. This results in excessive spike synchronization to β phase in Globus Pallidus interna (GPi) and STN³⁶, and excessive coherence between these basal ganglia nuclei and the motor cortex, which may drive M1 spiking and synaptic activity to have abnormally increased coupling to the phase of β rhythms. This aberrant PAC could constrain neurons in an inflexible pattern of activity, resulting in parkinsonian motor signs. The results of the present study provide further evidence for an important role for cortical PAC in the pathophysiology of Parkinson's disease since a therapy that improves motor signs, also reduces exaggerated PAC, with a similar time course. However, the causal relation between PAC and specific motor signs and symptoms of PD remains to be established.

Role of DBS in movement related PAC changes

In the motor cortex in the normal state, β -broadband activity PAC is strongly reduced during both movement preparation and execution^{22, 23}. The high PAC state may suppress cortical information processing at rest and its cessation before movement onset may induce a shift to an active processing state²³. Our results show that although Parkinson's disease patients could accomplish this transition, it was facilitated by therapeutic DBS, which reduced PAC at each phase of movement. We propose that elevated PAC in the resting state and during movement preparation is associated with akinesia and rigidity, while elevated PAC during movement execution is associated with bradykinesia. Chronic STN DBS might improve these symptoms by reducing the excessive PAC in all conditions.

PAC reduction by DBS is not solely due to β power changes

One current working hypothesis for the mechanism of DBS is suppression of basal ganglia oscillatory activity especially in the β band (13-30 Hz). This hypothesis is derived largely from recordings of local field potentials in the STN of Parkinson's disease patients, that have shown a prominent β oscillation that is reduced by therapeutic medications and by therapeutic DBS in a manner that correlates with symptom improvement^{2, 3, 5-8, 37}. However, to date, there is no consistent evidence of increased narrow band β power in the motor cortex of Parkinson's disease patients off medication compared to non-parkinsonian subjects, nor to Parkinson's disease patients on medication^{11, 13, 38} (although there is an increase in broadband activity in PD³⁸). In one prior paper using ECoG in Parkinson's disease, Whitmer et al. (2012) found an attenuation of β power during acute STN DBS in the motor cortex of two of the three patients tested. Here, with anatomically similar electrode placement in a much larger sample size, we found that DBS in individual subjects produced modest decreases or increases in β power without consistent change in grouped data. Our findings indicate that entrainment of population spiking and synaptic activity to the β rhythm, as measured by β phase-broadband amplitude coupling, may be a more sensitive method to measure the parkinsonian state and the effectiveness of therapeutic intervention.

Entrainment of subcortical axonal firing and reduction of cortical PAC

DBS is thought to partially entrain action potential firing in axons in close proximity to the stimulating electrode, which may be either afferent or efferent with respect to the stimulated nucleus³⁹⁻⁴¹. Axonal antidromic spikes evoked by STN DBS strongly affect the firing

probability of cortical neurons, inducing short periods of inhibition and excitation⁴²⁻⁴⁴. This DBS-generated pattern of firing probability, if present at the optimal frequency, could decouple the strong dependence of spike firing on β phase in M1 by increasing neuronal noise⁴⁵. The proposed mechanism has to be verified by actually measuring M1 single units, since in this study we used broadband activity as a surrogate measure of neuronal activity. However, antidromic activation of corticosubthalamic neurons is probably not the only mechanism by which DBS acts to reduce the excessive cortical synchronization observed in Parkinson's disease patients, since DBS at other basal ganglia targets that lack direct cortical connections like the globus pallidus interna, are also effective for symptom alleviation⁴⁶. The stimulation-induced β power reduction observed in STN may also be causally linked to decreased cortical PAC, by reducing the β entrainment of spike discharge³⁶ through a polysynaptic pathway connecting STN to cortex via the GPi and motor thalamus.

Implications for improved therapy

The reduction in cortical PAC by DBS implies that PAC could be used as a control signal for a “closed-loop” DBS device. This “smart” DBS device would record cortical activity, quickly compute PAC and determine computationally how to stimulate subcortical structures in a manner that best minimizes abnormal network activity. Development of closed-loop DBS devices will have an important impact in the treatment of movement disorders by overcoming the main limits of the current therapy such as the labor-intensive programming based on frequent symptom assessment by clinicians, stimulation induced adverse effects, the habituation (less efficacy over time), and short battery life. Two alternative approaches to the development of closed loop stimulation devices have been proposed, one utilizing cortical single unit activity and another utilizing STN LFP β oscillations^{47, 48}. Implementation of these strategies in a fully implantable closed loop system may be hampered by the risk of injury and lack of signal stability of cortical unit recording for the former approach, and by the low signal to noise ratio and high susceptibility to stimulation artifact for the latter. Our work suggests a strategy to overcome these issues by measuring the neuronal synchronization (using phase-amplitude coupling) at the cortical level. This approach would use high amplitude signals with minimal stimulation artifact, and a recording electrode that does not penetrate brain tissue. This strategy may also be generalized to other neurologic or psychiatric diseases. However, each potential control strategy (cortical versus basal ganglia) has its own advantages and shortcomings, and each ones should be explored.

Limitations

This study was limited by the temporal and logistical constraints of human intraoperative studies. Therefore, only brief recordings were collected; 30 seconds to 1 minute for the rest condition, and each patient performed only 10 to 20 trials of the arm movement task in each DBS condition, lasting on average 5 minutes. In addition, data used in this study were collected after insertion of the DBS lead in the STN, which is known to cause edema around the lead tip and can result in symptom improvement⁴⁹. Sedatives given for surgical exposure, although stopped 1-3 hours prior to recording, may also influence the intraoperative recordings and task performance. Moreover, the time for the effect of stimulation to wash in is variable and only one set of stimulation parameters was used.

Therefore, it is likely that the maximal effect of DBS was not reached in most patients. Arm rigidity is a motor sign that responds reliably to acute intraoperative DBS, but restrictions of the intraoperative environment did not allow for a precise characterization of rigidity beyond the UPDRS motor score, and this score lacks the sensitivity to infer a causal relationship between PAC reduction and improvement in motor function. Because of technical considerations, we did not investigate the effect of DBS on STN PAC. Indeed, PAC observed in STN of PD patients involved very high frequencies (>250Hz) that are filtered out by the online low pass filter (< 100 Hz) applied to avoid signals saturation.

Conclusion

In Parkinson's disease, acute therapeutic DBS acts on the cortex by reducing the excessive coupling between β oscillations and broadband activity, not only at rest but also during movement preparation and execution. Our results support the hypothesis that PAC is a biomarker of the parkinsonian state that could be used to improve DBS therapy by developing adaptive DBS devices.

Materials and methods

Patients

Patients were recruited from two centers; the movement disorders surgery clinics at the University of California, San Francisco (UCSF) or the San Francisco Veteran's Affairs Medical Center (SFVAMC). Patients included in this study had a diagnosis of idiopathic Parkinson's disease with mild to moderate bradykinesia/rigidity as predominant signs as attested by UPDRS III off medication score between 30 and 60, were scheduled to undergo DBS implantation in the awake state, and gave written informed consent. Motor impairment was assessed preoperatively by a movement disorders neurologists using the Unified Parkinson's Disease Rating Scale part III (UPDRS-III) in the off and on medication state. In addition, tremor and rigidity were assessed intraoperatively before each recording using UPDRS item 22 and 20, respectively. Patients were excluded if they had prominent tremor during recordings (UPDRS 20 \geq 3; 9 patients) or had a peak-to-peak M1 LFP amplitude of <50 microvolts at rest (4 patients). Twenty-three patients were included in this study. No statistical methods were used to pre-determine sample sizes but our sample sizes are similar to those reported in previous publications. The effect of DBS on STN was also studied in two of these patients and 3 additional patients (Table S6). This study was in agreement with the Declaration of Helsinki and was approved by the institutional ethics committee.

ECoG strip and lead location

Cortical local field potentials were recorded using a 6-contact electrocorticography (ECoG) strip temporarily placed over the sensori-motor cortex. The ECoG strip was inserted under the dura through the burr hole used for the DBS lead placement and advanced in the direction of the intended target location, the arm area of motor cortex (3 cm from the midline, slightly medial to the "hand knob"⁵⁰). Electrodes were composed of platinum contacts of 4 mm total diameter, 2.3 mm exposed diameter and 1 cm spacing between contacts (Ad-Tech, Racine, WI). Localization of the electrodes was confirmed anatomically,

using either intraoperative computed tomography (iCT) merged with pre-operative MRI or lateral fluoroscopy (Fig. 1a)⁵¹. In addition, somatosensory potentials evoked by median nerve stimulation were used to select the contact used for the subsequent analyses (frequency = 2Hz, pulse width = 200 µsec, pulse train length = 160 µsec, amplitude 25-40 mAmp). The most posterior contact showing a negative N20 waveform was defined as the closest electrode to M1.

DBS electrodes were placed in the STN as previously described⁵². The STN target was identified on a T2-weighted magnetic resonance image (MRI) as a signal hypointensity, lateral to the anterior margin of the red nucleus and superior to the lateral part of the substantia nigra pars reticulata. The STN target location was typically close to 12 mm lateral, 3 mm posterior, and 4 mm inferior to the midpoint of the line connecting the anterior and posterior commissures. Final adjustments on the target coordinates were made during the surgery based on identification of movement-related single cell discharge. Neurons exhibiting change in activity during arm movement ('arm cell'), leg movements ('leg cell') or in presence of tremor ('tremor cell') were identified. A DBS lead (model 3389 in 17 patients and 3387 in 6 patients, Medtronic, Inc., Minneapolis, Minnesota, USA) was then placed at these coordinates with the most ventral contact (contact 0) at the base of STN and contact 1 in the center of the motor territory of the STN. Targeting was confirmed by evaluation of stimulation induced symptom improvement and adverse effects, as well as by visualization of DBS lead location on an iCT scan computationally fused to the preoperative MRI⁵³(Fig. 1b).

Therapeutic stimulation parameters

STN was stimulated through the DBS lead (Medtronic model 3389) using an analog neurostimulator (Medtronic model 3625), in a bipolar configuration using a contact in the motor territory of STN as the active contact (contact1 in most patients) and a contact at the dorsal border of STN as the reference (contact 2 in most patients). Given that we did not search for optimal settings before the recordings, stimulation parameters were set at higher voltage (4 Volts) than these often used for chronic stimulation (see Table 1 for individual subject parameters), and at a typical therapeutic stimulation frequency (140-210 Hz). Further, routine clinical test stimulation was deferred until after the experimental data were collected, so as to avoid lingering effects of stimulation performed prior to the experimental paradigm. Changes in the clinical symptoms were determined in most patients and most conditions by assessment of contralateral limb rigidity and tremor using the UPDRS scale, item III 22 and item III 20, respectively (Table 1). We focused on rigidity rather than bradykinesia because it responds reliably to acute DBS and can be tested rapidly without the patient's full cooperation. Note that while patients with severe tremor were excluded from the study (UPDRS 20 = 3), 9 patients had mild tremor during experimental recordings (UPDRS 20 = 2). Given the constrain of intraoperative studies symptoms were assessed by unblinded neurologists in most cases. However, in order to reduce this bias, different stimulation settings (therapeutic and non-therapeutic) in a randomized paradigm, with motor evaluation by a blinded neurologist.

Cortical and LFP recordings

ECoG potentials were recorded in a bipolar configuration referencing the five most posterior contacts (contacts 1-5) to the most anterior one (contact 6) and using a needle electrode in the scalp as the ground. Signals were bandpass filtered 1-500 Hz, amplified $\times 7000$. LFPs were recorded using the Alpha Omega Microguide Pro (Alpha Omega, Inc, Nazareth, Israel) (18 patients) or the customized clinical recording systems, the Guideline 4000 system (FHC Inc, Bowdoin, ME) (5 patients). LFPs were recorded at a sampling rate of minimum 1000 Hz and up to 3000 Hz. All antiparkinsonian medications were stopped 12 hours before the start of surgery. All data were recorded 5 to 60 minutes after lead insertion in order to minimize the confounding effect of temporary 'microlesion' associated caused by lead insertion^{54, 55}. All but one patient underwent surgery for bilateral STN implantation. In bilateral DBS implantation surgeries, we deliberately recorded brain activity on the second side implanted, so to allow more time between the cessation of propofol sedation, and the start of ECoG recording for this study. Fig. 1d represents the typical timeline for stimulation and recording. To avoid lingering effects of stimulation, experimental conditions were not randomly selected but data were rather collected in the following sequence; First, 'before DBS' was collected and evaluated after lead insertion, before any stimulation. Second, 'during DBS' was collected when DBS turned on for the first time, before searching for optimal contact and stimulation parameters. Third, 'after DBS' was collected after DBS turned off for several minutes.

Behavioral paradigms

Two behavioral states were used. In all subjects, ECoG potentials were recorded before, during and after acute STN stimulation while the patient was relaxing, with eyes open, fixating on a point approximately 1 meter away, for at least 30 seconds (rest condition). Twelve of these patients performed an arm movement task in the three different stimulation conditions. The task was designed to study the effect of DBS not only on movement execution but also on its preparation (Fig.1c). Each trial started with a 'hold' period of 5-7 s during which the subject was asked to rest his hand on his lap, while maintaining gaze on a central red dot. Then, the 'target', a blue dot, occurred at the upper or lower edge of the screen. The position of the target was randomly chosen as either the upper and lower edge of the screen. A change of color from red to green ('go' signal) instructed the patient to touch with the index finger the target that will then step vertically from one position to the other (usually 5 steps). During the move phase, patients perform a continuous movement for about 3s. The duration between the target onset and the go signal was 3-5s depending on patient ability. Patients performed ten to twenty trials in all stimulation conditions. The task was performed on a mobile device (iPad, Apple computer). This task allow us to distinguish 3 phases: The hold phase, the movement preparation phase and the movement execution phase. Movement kinematics were measured both by electromyography (EMG) of extensor carpi radialis, flexor carpi radialis and biceps brachii (bandpass filter 1-1000 Hz, amplification $\times 7000$, sampling rate of 1 to 3 KHz) as well as a tri-axial accelerometry wrist band (AX2300-365, FHC, Inc, Bowdoin, ME). Movement onset and offset were identified as periods during which accelerometry and EMG exceed a threshold defined as two standard deviations above the mean EMG and accelerometry computed during the hold phase of each trial.

Signal processing and analyses

In order to obtain a better spatial localization and reduced noise, LFPs recorded from each contact were re-referenced to its posterior adjacent contact (C1-C2, C2-C3...). Ambient noise (60Hz and harmonics) was rejected off line using a notch filter (Butterworth filter, bandwidth=4 Hz, order=3). Given the distance between stimulation and recording sites and/or the bipolar montage used to analyze the data, the stimulation artifact was small relative to the cortical signal, in most recordings (Fig. 2). However, stimulation artifact was filtered out using a notch filter (Butterworth filter, bandwidth=4 Hz, order=3). This filtering procedure was applied in all conditions (before, during and after stimulation). However, in order to examine whether the stimulation artifact affected results, this filtering procedure was not applied for Supplementary Fig. 2. LFPs recorded with a frequency sampling greater than 1000 Hz were down sampled to 1000 Hz. For data recorded at rest, the first 30s of data without obvious electrical noise or movement were selected for the analyses. For data recorded during the task, trials during which the subject initiated movement before the go signal were excluded from the analyses. In order to study the effect of task phase, time series data were separated into hold, preparation and movement phases. Each phase was then subdivided into 1 second segments that were used for analyses (PSD and PAC see below) then averaged across phases. All analyses were performed using Matlab 7.10 software (Mathworks). Data collection and analysis were not performed blind to the conditions of the experiments.

In the resting condition, *Power spectral density* (PSD) was calculated with the Welch periodogram method (Matlab function `pwelch`) using a fast Fourier transform of 512 points (frequency resolution of 1.95 Hz), and 50% overlap, using a Hanning window to reduce edge effects. PSD was computed in the three conditions of stimulation and was transformed in logarithm scale and used for all statistical comparisons to allow for use of parametric tests. Four variables were extracted from the log PSD; the “ β peak” defined as the maximum value between 13 and 30 Hz; the “ β peak frequency” defined as the frequency at which the “ β peak” occurred, “log β power” defined as the average of the log PSD across the β band (13-30 Hz) and “log γ power” defined as the average of the log PSD across the broadband activity (50-200 Hz).

In the task, cortical changes related to movement preparation and movement initiation were studied using time frequency analysis. Cortical power spectral density was computed using the short time Fourier transform (`spectrogram`; MATLAB function) with a 512-point window and 50 sample (50 ms) frame advance. PSDs were aligned on either on the ‘target’ occurrence, corresponding to the end of the hold phase, or on the movement onset. Each frequency of the PSD was then normalized to the baseline defined as the PSD averaged across 1 sec prior to target onset. Four variables were then computed: ‘ β changes prep’ and ‘broadband power changes prep’ were determined by averaging the time spectrograms across a period from 1sec before to the ‘go’ signal in the β band (13-30Hz) and broadband activity (50-200Hz), respectively, ‘ β changes mvt’ and ‘broadband power changes mvt’ were determined by averaging the time spectrograms across 1sec at movement onset in the β band (13-30Hz) and broadband activity (50-200Hz), respectively. Each variable was expressed as the percentage of changes from baseline.

Phase-amplitude coupling indices were quantified using a method previously described⁵⁶. First, ECoG potentials were bandpass filtered at low (from 4 to 50 Hz in 2Hz steps with a 2Hz bandwidth, without overlap) and high frequency (from 50 to 200 Hz in 4Hz steps with a 4Hz bandwidth, without overlap) using a FIR1 filter (eeglab). Second, the instantaneous phase and the instantaneous amplitude were extracted from the low and the high frequency filtered signal, respectively, after applying the Hilbert transform. The instantaneous phase was divided into bins of 20° and a distribution of the instantaneous amplitude envelope was computed for each bin. The phase-amplitude coupling was then determined by computing the entropy values of this distribution and normalizing by the maximum entropy value. Coupling was computed for multiple frequencies for phase and amplitude represented on a modulation index plot (Fig 3a). This method was selected because it is less sensitive to noise, independent to the amplitude of the raw signal, does not require visible peaks in power spectra, is sensitive to the intensity of cross-frequency coupling and can detect multimodal phase-amplitude coupling (additional method were used in supplementary section^{57, 58}). Tasks and treatments have been shown to affect not only the magnitude of PAC but also the phase at which the coupling occurs and the frequencies (phase and amplitude) involved in this interaction^{59, 60}. Therefore, for each frequency pair, the phase of the coupling (“preferred phase”) was calculated by determining the phase at which the instantaneous amplitude was maximal. For each patient and each stimulation condition, the overall magnitude (*PAC mean*) of β -broadband activity coupling was determined by averaging the coupling between phases extracted from the 13-30 Hz band and the amplitude extracted from the 50-200 Hz band. The ‘mean preferred phase’ was computed by averaging the ‘preferred phase’ computed frequency for phase between 13-30 Hz band and frequency for amplitude between 50-200 Hz band (*circ_mean.m* from the circular statistics toolbox). In addition, the frequencies involved in the maximal coupling (*PAC freq phase* and *PAC freq amp*) were determined.

Between groups statistical analysis

Statistical analyses were performed in SPSS and Matlab, using paired non parametric tests given the non-normal distribution of most variables studied (Ranktest, Ranksign test, Friedman test and spearman correlation).

Supplementary Material

Refer to Web version on PubMed Central for supplementary material.

Acknowledgments

Thanks to our patients who participated in this study, to Richard Steiner for programming the iPad task, to Anatol Kreitzer for critical review of the manuscript, to Svyetlana Miocinovic for patients symptoms assessment, to Nathan Ziman and Salman Qasim for helping in collecting data.

Funding: This study was supported by a grant from the Michael J. Fox foundation, and by NIH R01 NS069779.

References

1. Benabid AL, Chabardes S, Mitrofanis J, Pollak P. Deep brain stimulation of the subthalamic nucleus for the treatment of Parkinson's disease. *Lancet Neurol.* 2009; 8:67–81. [PubMed: 19081516]

2. Wingeier B, et al. Intra-operative STN DBS attenuates the prominent beta rhythm in the STN in Parkinson's disease. *Exp Neurol*. 2006; 197:244–251. [PubMed: 16289053]
3. Kuhn AA, et al. High-frequency stimulation of the subthalamic nucleus suppresses oscillatory beta activity in patients with Parkinson's disease in parallel with improvement in motor performance. *J Neurosci*. 2008; 28:6165–6173. [PubMed: 18550758]
4. Ray NJ, et al. Local field potential beta activity in the subthalamic nucleus of patients with Parkinson's disease is associated with improvements in bradykinesia after dopamine and deep brain stimulation. *Exp Neurol*. 2008; 213:108–113. [PubMed: 18619592]
5. Bronte-Stewart H, et al. The STN beta-band profile in Parkinson's disease is stationary and shows prolonged attenuation after deep brain stimulation. *Exp Neurol*. 2009; 215:20–28. [PubMed: 18929561]
6. Rossi L, et al. Subthalamic local field potential oscillations during ongoing deep brain stimulation in Parkinson's disease. *Brain Res Bull*. 2008; 76:512–521. [PubMed: 18534260]
7. Eusebio A, et al. Deep brain stimulation can suppress pathological synchronisation in parkinsonian patients. *J Neurol Neurosurg Psychiatry*. 2010
8. Whitmer D, et al. High frequency deep brain stimulation attenuates subthalamic and cortical rhythms in Parkinson's disease. *Front Hum Neurosci*. 2012; 6:155. [PubMed: 22675296]
9. Stoffers D, et al. Slowing of oscillatory brain activity is a stable characteristic of Parkinson's disease without dementia. *Brain*. 2007; 130:1847–1860. [PubMed: 17412733]
10. Melgari JM, et al. Alpha and beta EEG power reflects L-dopa acute administration in parkinsonian patients. *Frontiers in aging neuroscience*. 2014; 6:302. [PubMed: 25452725]
11. Litvak V, et al. Resting oscillatory cortico-subthalamic connectivity in patients with Parkinson's disease. *Brain*. 2011; 134:359–374. [PubMed: 21147836]
12. Hirschmann J, et al. Distinct oscillatory STN-cortical loops revealed by simultaneous MEG and local field potential recordings in patients with Parkinson's disease. *Neuroimage*. 2011; 55:1159–1168. [PubMed: 21122819]
13. de Hemptinne C, et al. Exaggerated phase-amplitude coupling in the primary motor cortex in Parkinson disease. *Proc Natl Acad Sci U S A*. 2013
14. Manning JR, Jacobs J, Fried I, Kahana MJ. Broadband shifts in local field potential power spectra are correlated with single-neuron spiking in humans. *J Neurosci*. 2009; 29:13613–13620. [PubMed: 19864573]
15. Suffczynski P, Crone NE, Franaszczuk PJ. Afferent inputs to cortical fast-spiking interneurons organize pyramidal cell network oscillations at high-gamma frequencies (60-200 Hz). *J Neurophysiol*. 2014; 112:3001–3011. [PubMed: 25210164]
16. Canolty RT, Knight RT. The functional role of cross-frequency coupling. *Trends Cogn Sci*. 2010; 14:506–515. [PubMed: 20932795]
17. Jacobs J, Kahana MJ, Ekstrom AD, Fried I. Brain oscillations control timing of single-neuron activity in humans. *J Neurosci*. 2007; 27:3839–3844. [PubMed: 17409248]
18. Axmacher N, et al. Cross-frequency coupling supports multi-item working memory in the human hippocampus. *Proc Natl Acad Sci U S A*. 2010; 107:3228–3233. [PubMed: 20133762]
19. Canolty RT, et al. High gamma power is phase-locked to theta oscillations in human neocortex. *Science*. 2006; 313:1626–1628. [PubMed: 16973878]
20. Cohen MX, Elger CE, Fell J. Oscillatory activity and phase-amplitude coupling in the human medial frontal cortex during decision making. *J Cogn Neurosci*. 2009; 21:390–402. [PubMed: 18510444]
21. Voytek B, et al. Shifts in gamma phase-amplitude coupling frequency from theta to alpha over posterior cortex during visual tasks. *Front Hum Neurosci*. 2010; 4:191. [PubMed: 21060716]
22. Yanagisawa T, et al. Regulation of motor representation by phase-amplitude coupling in the sensorimotor cortex. *J Neurosci*. 2012; 32:15467–15475. [PubMed: 23115184]
23. Miller KJ, et al. Human motor cortical activity is selectively phase-entrained on underlying rhythms. *PLoS Comput Biol*. 2012; 8:e1002655. [PubMed: 22969416]

24. Purzner J, et al. Involvement of the basal ganglia and cerebellar motor pathways in the preparation of self-initiated and externally triggered movements in humans. *J Neurosci.* 2007; 27:6029–6036. [PubMed: 17537974]
25. Kuhn AA, et al. Event-related beta desynchronization in human subthalamic nucleus correlates with motor performance. *Brain.* 2004; 127:735–746. [PubMed: 14960502]
26. Williams D, et al. The relationship between oscillatory activity and motor reaction time in the parkinsonian subthalamic nucleus. *Eur J Neurosci.* 2005; 21:249–258. [PubMed: 15654862]
27. Temel Y, et al. Differential effects of subthalamic nucleus stimulation in advanced Parkinson disease on reaction time performance. *Exp Brain Res.* 2006; 169:389–399. [PubMed: 16273395]
28. Lopez-Azcarate J, et al. Coupling between beta and high-frequency activity in the human subthalamic nucleus may be a pathophysiological mechanism in Parkinson's disease. *J Neurosci.* 2010; 30:6667–6677. [PubMed: 20463229]
29. Ozkurt TE, et al. High frequency oscillations in the subthalamic nucleus: A neurophysiological marker of the motor state in Parkinson's disease. *Exp Neurol.* 2011; 229:324–331. [PubMed: 21376039]
30. Eusebio A, et al. Effects of low-frequency stimulation of the subthalamic nucleus on movement in Parkinson's disease. *Exp Neurol.* 2008; 209:125–130. [PubMed: 17950279]
31. Crone NE, et al. Functional mapping of human sensorimotor cortex with electrocorticographic spectral analysis. I. Alpha and beta event-related desynchronization. *Brain.* 1998; 121(Pt 12): 2271–2299. [PubMed: 9874480]
32. Crone NE, Miglioretti DL, Gordon B, Lesser RP. Functional mapping of human sensorimotor cortex with electrocorticographic spectral analysis. II. Event-related synchronization in the gamma band. *Brain.* 1998; 121(Pt 12):2301–2315. [PubMed: 9874481]
33. Lakatos P, Karmos G, Mehta AD, Ulbert I, Schroeder CE. Entrainment of neuronal oscillations as a mechanism of attentional selection. *Science.* 2008; 320:110–113. [PubMed: 18388295]
34. Tort AB, et al. Dynamic cross-frequency couplings of local field potential oscillations in rat striatum and hippocampus during performance of a T-maze task. *Proc Natl Acad Sci U S A.* 2008; 105:20517–20522. [PubMed: 19074268]
35. Tort AB, Komorowski RW, Manns JR, Kopell NJ, Eichenbaum H. Theta-gamma coupling increases during the learning of item-context associations. *Proc Natl Acad Sci U S A.* 2009; 106:20942–20947. [PubMed: 19934062]
36. Moran A, Bergman H, Israel Z, Bar-Gad I. Subthalamic nucleus functional organization revealed by parkinsonian neuronal oscillations and synchrony. *Brain.* 2008; 131:3395–3409. [PubMed: 18986993]
37. Pogosyan A, et al. Parkinsonian impairment correlates with spatially extensive subthalamic oscillatory synchronization. *Neuroscience.* 2010; 171:245–257. [PubMed: 20832452]
38. Crowell AL, et al. Oscillations in sensorimotor cortex in movement disorders: an electrocorticography study. *Brain.* 2012; 135:615–630. [PubMed: 22252995]
39. Gradinaru V, Mogri M, Thompson KR, Henderson JM, Deisseroth K. Optical deconstruction of parkinsonian neural circuitry. *Science.* 2009; 324:354–359. [PubMed: 19299587]
40. Hashimoto T, Elder CM, Okun MS, Patrick SK, Vitek JL. Stimulation of the subthalamic nucleus changes the firing pattern of pallidal neurons. *J Neurosci.* 2003; 23:1916–1923. [PubMed: 12629196]
41. Vitek JL, Zhang J, Hashimoto T, Russo GS, Baker KB. External pallidal stimulation improves parkinsonian motor signs and modulates neuronal activity throughout the basal ganglia thalamic network. *Exp Neurol.* 2012; 233:581–586. [PubMed: 22001773]
42. Dejean C, Hyland B, Arbuthnott G. Cortical effects of subthalamic stimulation correlate with behavioral recovery from dopamine antagonist induced akinesia. *Cereb Cortex.* 2009; 19:1055–1063. [PubMed: 18787234]
43. Kuriakose R, et al. The nature and time course of cortical activation following subthalamic stimulation in Parkinson's disease. *Cereb Cortex.* 2010; 20:1926–1936. [PubMed: 20019146]
44. Li Q, et al. Therapeutic deep brain stimulation in parkinsonian rats directly influences motor cortex. *Neuron.* 2012; 76:1030–1041. [PubMed: 23217750]

45. Voytek B, Gazzaley A. Stimulating the aging brain. *Ann Neurol.* 2013; 73:1–3. [PubMed: 23378322]
46. Follett KA, et al. Pallidal versus subthalamic deep-brain stimulation for Parkinson's disease. *The New England journal of medicine.* 2010; 362:2077–2091. [PubMed: 20519680]
47. Little S, et al. Adaptive deep brain stimulation in advanced Parkinson disease. *Ann Neurol.* 2013
48. Rosin B, et al. Closed-loop deep brain stimulation is superior in ameliorating parkinsonism. *Neuron.* 2011; 72:370–384. [PubMed: 22017994]
49. Koop MM, Andrzejewski A, Hill BC, Heit G, Bronte-Stewart HM. Improvement in a quantitative measure of bradykinesia after microelectrode recording in patients with Parkinson's disease during deep brain stimulation surgery. *Mov Disord.* 2006; 21:673–678. [PubMed: 16440333]
50. Yousry TA, et al. Localization of the motor hand area to a knob on the precentral gyrus. A new landmark. *Brain.* 1997; 120(Pt 1):141–157. [PubMed: 9055804]
51. Crowell AL, et al. Oscillations in sensorimotor cortex in movement disorders: an electrocorticography study. *Brain.* 2012; 135:615–630. [PubMed: 22252995]
52. Starr PA, et al. Implantation of deep brain stimulators into the subthalamic nucleus: technical approach and magnetic resonance imaging-verified lead locations. *Journal of neurosurgery.* 2002; 97:370–387. [PubMed: 12186466]
53. Shahlaie K, Larson PS, Starr PA. Intra-operative CT for DBS surgery: technique and accuracy assessment. *Neurosurgery.* 2011; 68:114–124. [PubMed: 21206322]
54. Mann JM, et al. Brain penetration effects of microelectrodes and DBS leads in STN or GPi. *J Neurol Neurosurg Psychiatry.* 2009; 80:794–797. [PubMed: 19237386]
55. Tykocki T, Nauman P, Koziara H, Mandat T. Microlesion effect as a predictor of the effectiveness of subthalamic deep brain stimulation for Parkinson's disease. *Stereotactic and functional neurosurgery.* 2013; 91:12–17. [PubMed: 23154788]
56. Tort AB, et al. Dynamic cross-frequency couplings of local field potential oscillations in rat striatum and hippocampus during performance of a T-maze task. *Proc Natl Acad Sci U S A.* 2008; 105:20517–20522. [PubMed: 19074268]
57. Osipova D, Hermes D, Jensen O. Gamma power is phase-locked to posterior alpha activity. *PLoS One.* 2008; 3:e3990. [PubMed: 19098986]
58. Penny WD, Duzel E, Miller KJ, Ojemann JG. Testing for nested oscillation. *J Neurosci Methods.* 2008; 174:50–61. [PubMed: 18674562]
59. Lopez-Azcarate J, et al. Coupling between beta and high-frequency activity in the human subthalamic nucleus may be a pathophysiological mechanism in Parkinson's disease. *J Neurosci.* 2010; 30:6667–6677. [PubMed: 20463229]
60. Ozkurt TE, et al. High frequency oscillations in the subthalamic nucleus: A neurophysiological marker of the motor state in Parkinson's disease. *Exp Neurol.* 2011; 229:324–331. [PubMed: 21376039]

Abbreviations

DBS	deep brain stimulation
STN	subthalamic nucleus
LFP	local field potential
ECoG	electrocorticography
PAC	phase-amplitude coupling
EMG	electromyography
MRI	magnetic resonance imaging
PSD	power spectral density

UPDRS	Unified Parkinson's Disease Rating Scale
M1	primary motor cortex
iCT	intraoperative computed tomography
SSEP	somatosensory evoked potential

Author Manuscript

Author Manuscript

Author Manuscript

Author Manuscript

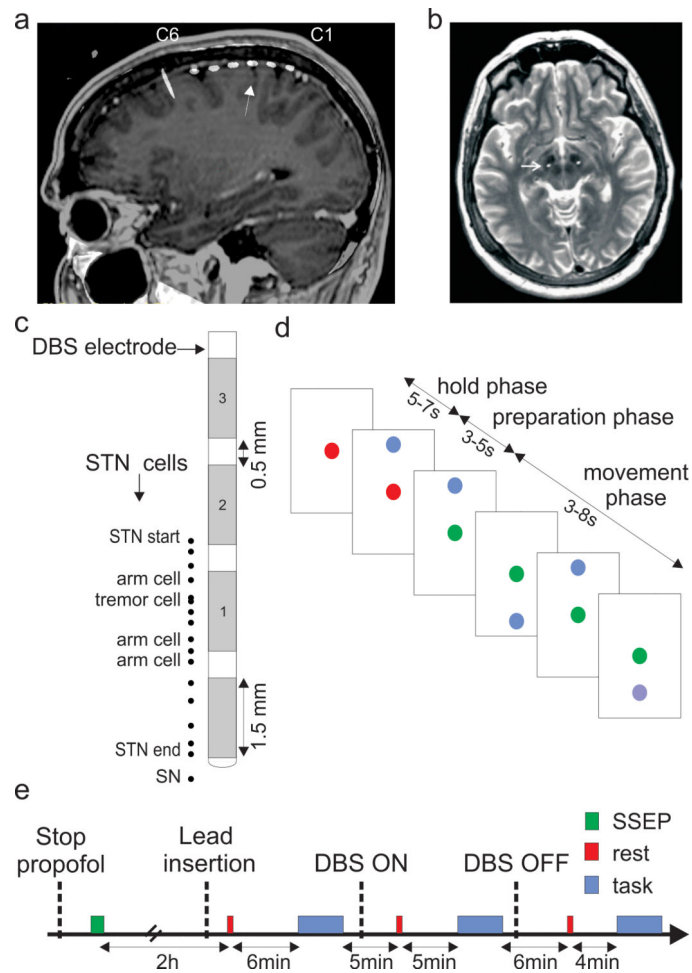
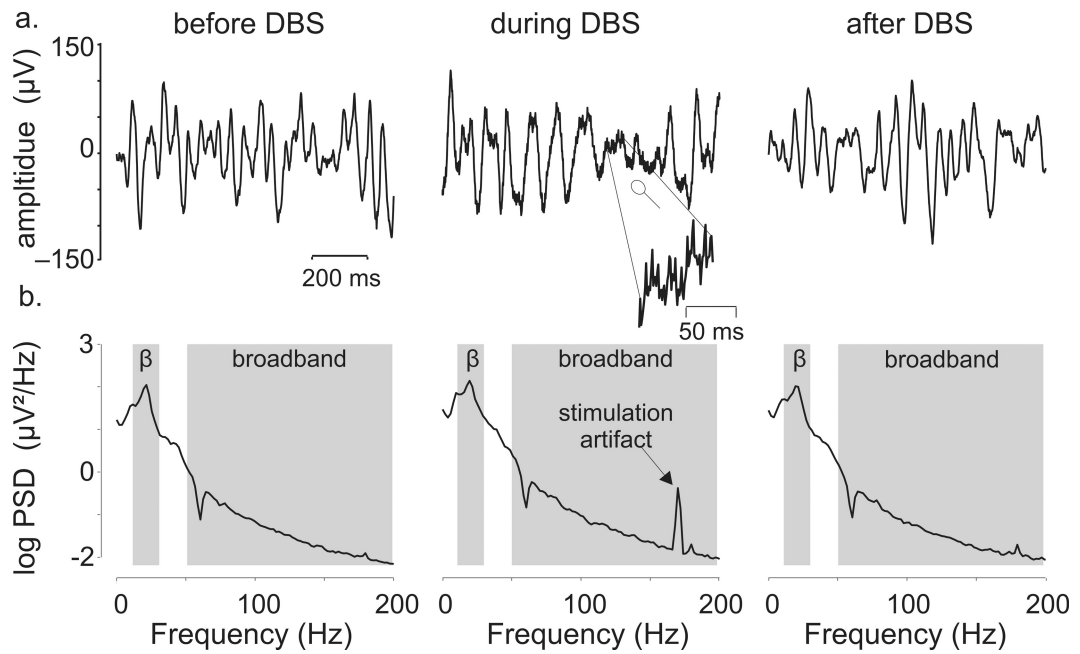
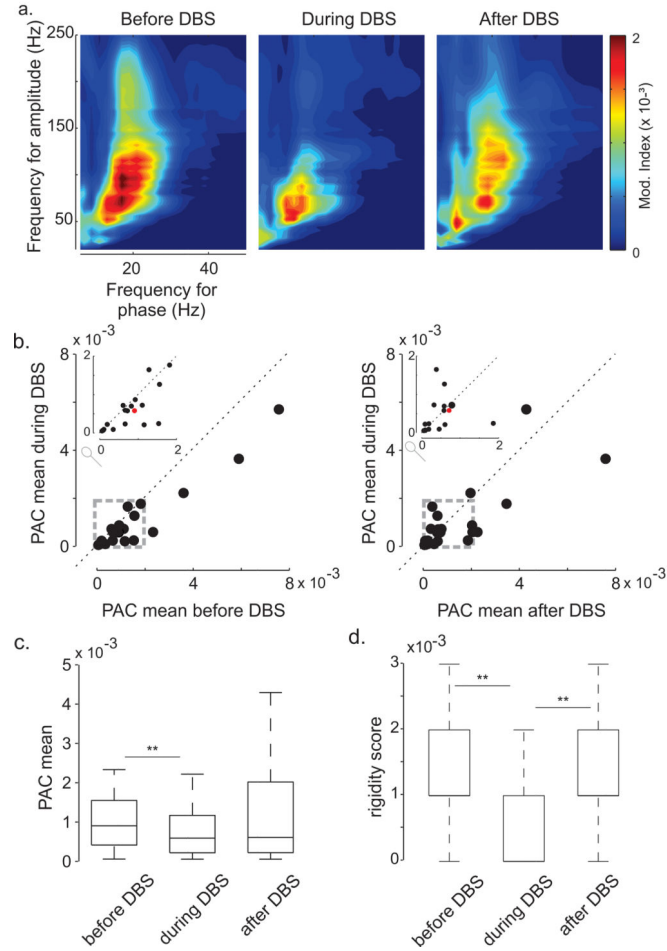


Fig.1. Electrodes localization, task paradigm, and timeline of recordings. **a.** Localization of subdural ECoG strip. The six contacts of the ECoG strip (white dots) relative to the central sulcus (*white arrow*) can be observed on this parasagittal view of the iCT scan merged with the preoperative MRI scan. **b.** Localization of tip of the DBS electrode (*arrow*) at the base of STN, on an axial view of the iCT scan merged with the preoperative MRI. **c.** Description of the arm movement task. A single trial is represented. Each trial starts with a ‘hold phase’ period of 3-5 s during which the patient maintains gaze on a central red dot. Then, the ‘target’, a blue dot, occurs at the upper or lower edge of the screen (‘preparation phase’). Patient was instructed to touch the target with the index finger after the central dot turns green (‘movement phase’). **d.** Typical timeline for lead insertion, recording, and stimulation. Rectangles represent the different data collection events as follows: Green, somatosensory evoked potential (SSEP); red, rest; blue; arm movement task. The time between recordings is indicated under the horizontal arrows in minutes or hour.

**Fig.2.**

Example M1 recordings and their spectral characteristics, prior to filtering the stimulation artifact, in a single patient. **a.** M1 LFPs before (*left panel*), during (*middle panel*) and after STN stimulation (*right panel*). **b.** Log power spectral density for each recording in (**a**). A small artifact of stimulation can be observed on the zoomed LFP (**a middle panel**) and the corresponding log PSD (*arrow, b middle panel*). A peak in the β band can be observed in each condition. Grey rectangles indicate β band and broadband activity.

**Fig.3.**

Acute therapeutic STN stimulation reduces PAC in the resting state. a. Representative example of PAC observed in the M1 of a Parkinson's disease patient before (left panel), during (middle panel) and after STN stimulation (right panel). The warmest colors represent the strongest coupling. The white dotted box (left panel) shows the range of frequencies over which modulation indices were averaged to generate the statistical comparison between stimulation conditions. b. Average PAC observed during DBS is plotted versus that observed before DBS (left panel) and after DBS (right panel). Each dot represents one patient. Grey rectangles show the zoomed area plotted in the inserts. c. Boxplot showing the significant and partly reversible reduction of PAC during STN DBS. d. Boxplot showing the therapeutic reversible effect of DBS on patient's rigidity. The boxes represent the 25th and 75th percentiles, and the whiskers extend to the most extreme data points not considered outliers (1.5 IQR). * indicates a significant difference with a p-value <0.05 and ** with a p-values <0.01.

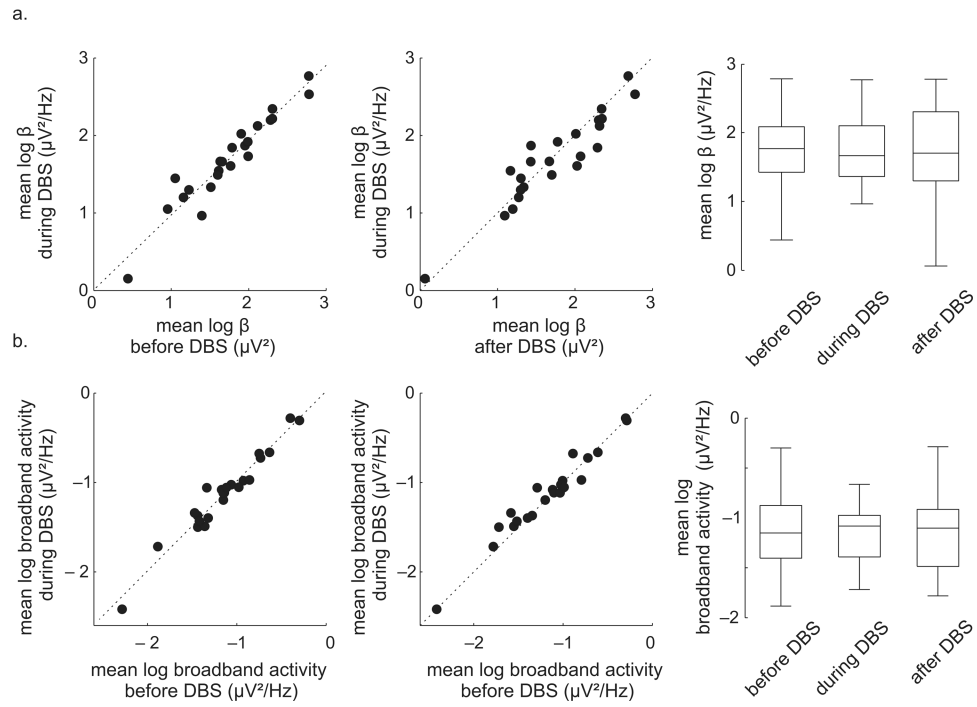


Fig. 4. DBS does not affect resting state power spectral density. **a.** Mean β power. For each subject before versus during DBS (*left*), for each subject after DBS versus during DBS (*middle*), and grouped data represented in boxplots (*right*). **b.** Mean broadband power, represented in same manner as in **a.** Same conventions as in Fig. 3d

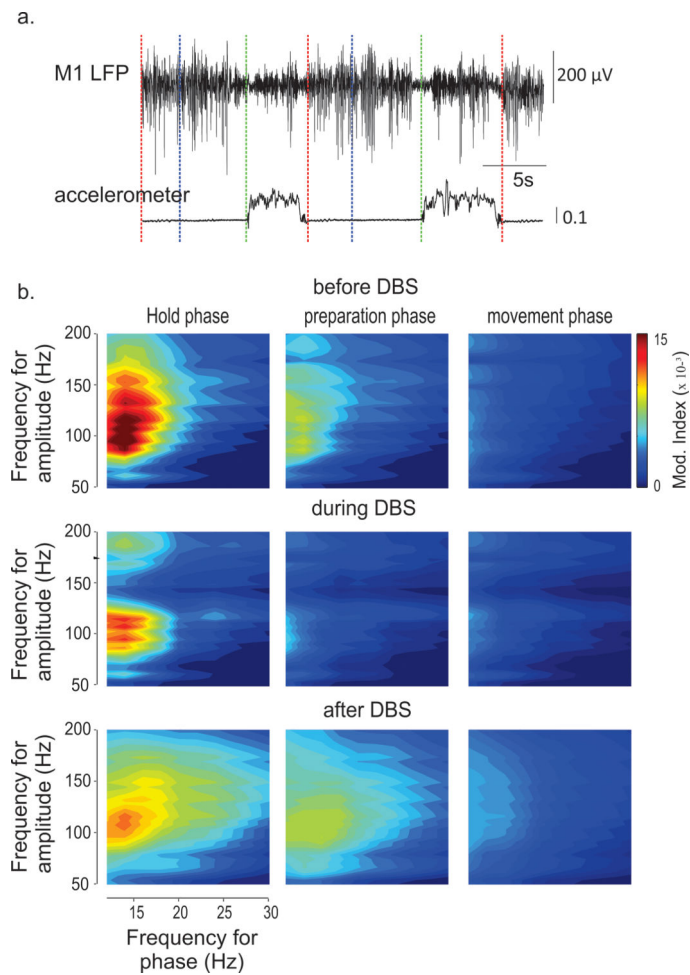


Fig. 5. Examples of M1 LFP and PAC during the arm movement task in one patient. **a.** M1 LFP (*top panel*) and accelerometry (*lower panel*) during two trials of the task. Vertical dashed lines indicate the three phases of the task: red; hold phase, blue; preparation, green; movement. **b.** PAC in the three phases (*left panels*, hold; *middle panels*, preparation; *right panels*, movement) and in the three conditions of stimulation (*top panels*, before DBS; *middle panels*, during DBS; *lower panels*, after DBS). There is reduction of PAC from hold to movement preparation to movement execution, and DBS decreases PAC in all three phases of the task.

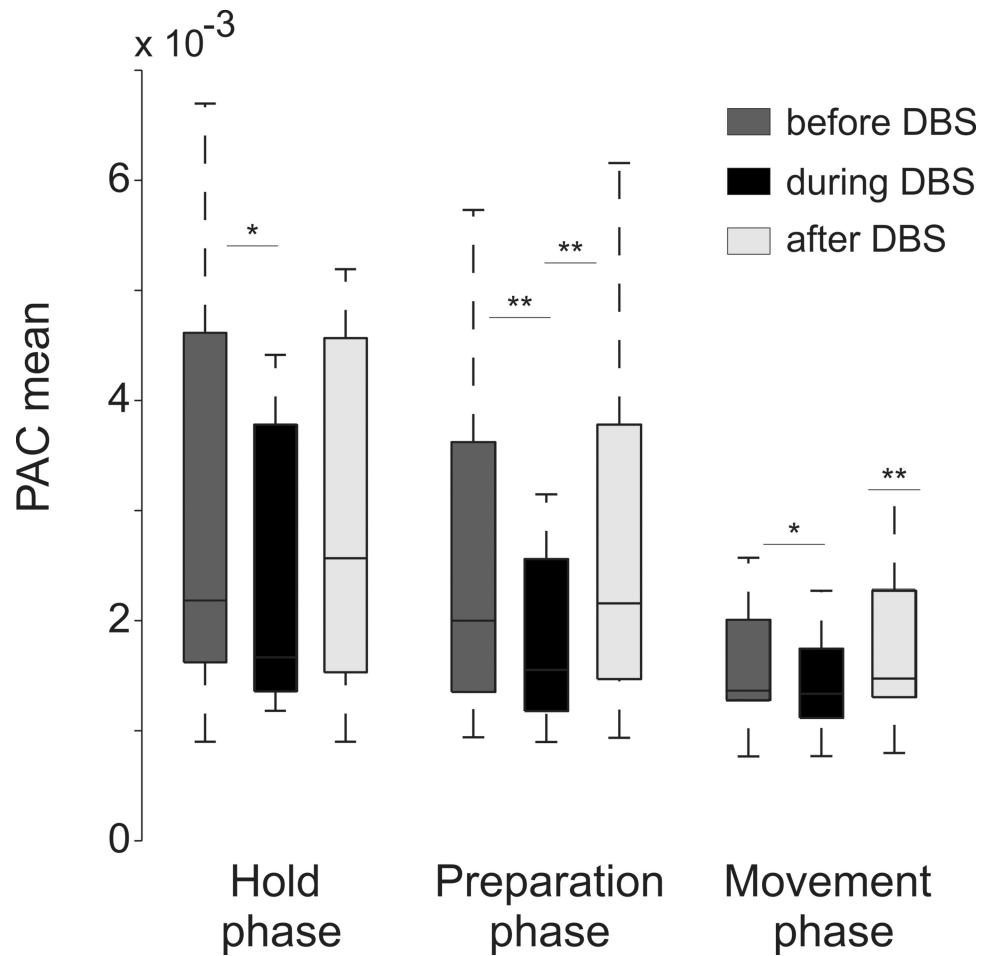


Fig. 6. Both DBS and movement reduce PAC during the arm movement task. Medians and 25-75 percentiles are shown in the three phases of the task (hold, preparation and movement) before and during DBS stimulation. The three phases are represented in the x axis while the conditions are represented by colors. *Dark grey*, before DBS; *black*, during DBS; *light grey*, after DBS. A reduction of PAC is observed from hold phase to movement phase with an additional decrease of PAC during STN stimulation. Same conventions as in Fig. 3d

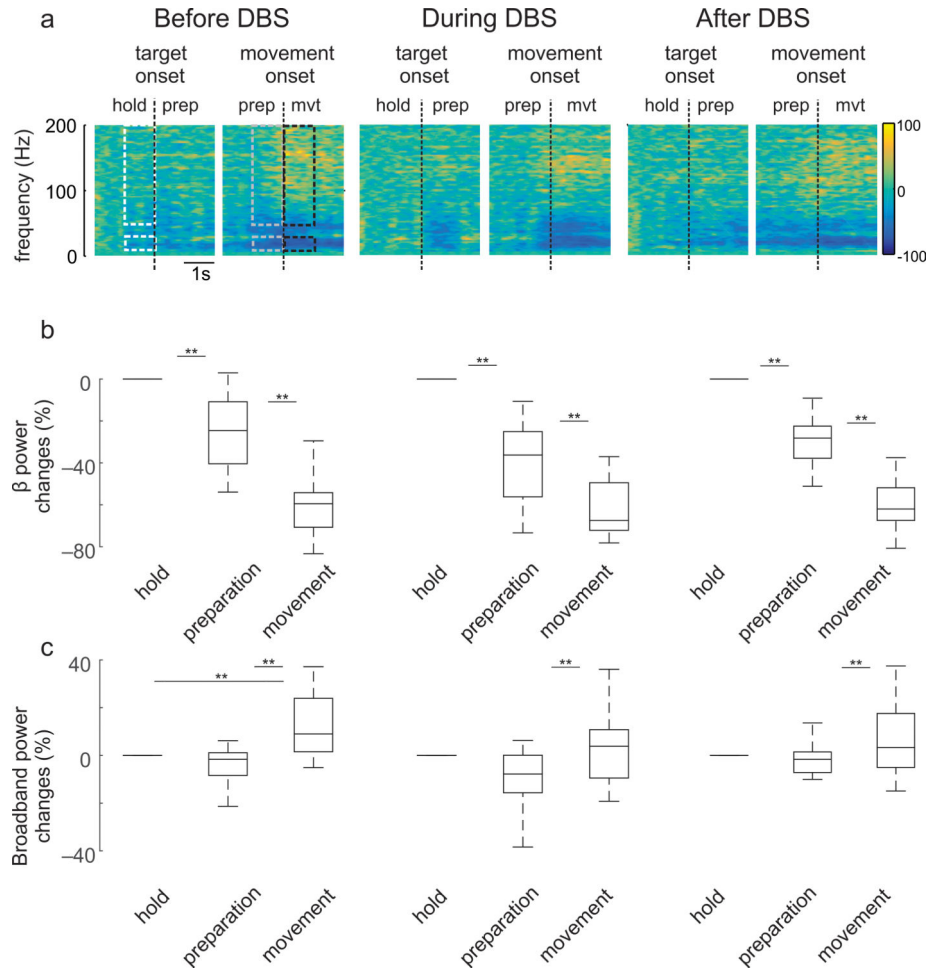


Fig.7. Movement related cortical changes before, during and after DBS. **a.** Typical example of cortical changes associated with movement preparation and initiation observed before (*left panel*), during (*middle panel*) and after DBS (*right panel*) in an individual patient (PD7). Time spectrograms are aligned either on the target onset (*dashed vertical line; left spectrograms*) or the movement onset (*dashed vertical line; right spectrograms*). Spectrograms were averaged across β frequency (13-30Hz) and broadband (100-200Hz), during the hold period (*white rectangles*), the preparation phase (*grey rectangles*) and the movement onset (*black rectangles*). **b.** Boxplots showing changes in β activity associated to movement preparation and execution before (*left panel*), during (*middle panel*) and after DBS (*right panel*). Significant p values are indicated. **c.** Boxplots showing changes in broadband activity associated with movement preparation and execution before (*left panel*), during (*middle panel*) and after DBS (*right panel*). Significant p values (after correction for multiple comparisons) are indicated. Same conventions as in Fig. 3d

Demographic and clinical characteristics of the patients. **a** Pre-op Unified Parkinson's Disease Rating Scale part III on/off medication score **b**. Parameters of stimulation: contacts used; frequency, voltage and pulse width. **c**. Intra-operative score for the arm contralateral to the cortical electrode and determined using the Unified Parkinson's Disease Rating Scale part III sub-item 22 and 20 for rigidity (*r*) and resting tremor (*t*).

Table 1

Pts	age	gender	ecog side	UPDRS III ON	UPDRS III OFF	Stimulation parameters	Score before DBS	Score during DBS	Score after DBS
PD1	54	M	L	23	42	1-2+, 155 Hz 4V 60 μ s	r = 2 t = 0	r = 0 t = 0	r = 2 t = 1
PD2	60	M	R	11	34	1-2+, 165 Hz 4V 60 μ s	r = 1 t = 1	r = 0 t = 0	r = 1 t = 0
PD3	54	M	L	9	21	0-2+, 186 Hz 4V 60 μ s	r = na t = 2	r = na t = 1	r = na t = na
PD4	68	M	R	30	50	1-2+, 170 Hz 4V 60 μ s	r = 2 t = 1	r = 1 t = 0	r = 2 t = 1
PD5	63	M	R	12	40	1-2+, 213 Hz 4V 60 μ s	r = 1 t = 0	r = 0 t = 0	r = na t = na
PD6	58	F	L	31	52	1-2+, 179 Hz 4V 60 μ s	r = 0 t = 0	r = 0 t = 0	r = 1 t = 0
PD7	57	M	L	10	31	1-2+, 168 Hz 4V 60 μ s	r = 0 t = 1	r = 0 t = 0	r = 0 t = 2
PD8	64	M	L	38	65	1-0+, 146 Hz 4V 60 μ s	r = 2 t = 1	r = 1 t = 0	r = 1 t = 0
PD9	63	M	R	32	48	1-2+, 155 Hz 4V 60 μ s	r = 2 t = 0	r = 1 t = 0	r = na t = na
PD10	53	M	R	11	30	1-2+, 143 Hz 4V 60 μ s	r = 1 t = 0	r = 0 t = 0	r = 1 t = 0
PD11	64	M	R	20	33	0-3+, 145 Hz 5V 60 μ s	r = 3 t = 1	r = 2 t = 1	r = 2 t = 2
PD12	61	F	L	21	40	1-2+, 138 Hz 4V 60 μ s	r = na t = 1	r = na t = 0	r = na t = na
PD13	64	M	L	23	33	1-2+, 144 Hz 4V 90 μ s	r = 0 t = 0	r = 0 t = 0	r = na t = na
PD14	76	M	L	18	50	0-3+, 130 Hz 4V 60 μ s	r = 1 t = 0	r = 0 t = 0	r = na t = na
PD15	65	F	L	17	30	0-3+, 140 Hz 4V 60 μ s	r = 3 t = 0	r = 2 t = 0	r = 3 t = 0
PD16	56	M	R	24	37	1-2+, 147 Hz 4V 60 μ s	r = 1 t = 1	r = 0 t = 0	r = 1 t = 0

Pts	age	gender	ecog side	UPDRS III ON	UPDRS III OFF	Stimulation parameters	Score before DBS	Score during DBS	Score after DBS
PD17	79	M	R	15	30	1-2+, 141 Hz 4V 60 μ s	r = na t = na	r = na t = na	r = na t = na
PD18	59	M	R	16	47	1-2+, 155 Hz 4V 60 μ s	r = 0 t = 0	r = 0 t = 0	r = 0 t = 1
PD19	74	M	R	27	48	1-2+, 195 Hz 4V 60 μ s	r = 0 t = 0	r = 0 t = 0	r = 0 t = 0
PD20	73	M	R	18	39	1-2+, 213 Hz 4V 60 μ s	r = 2 t = 0	r = 1 t = 0	r = na t = na
PD21	67	M	L	31	50	1-2+, 180 Hz 4V 60 μ s	r = 2 t = 0	r = 1 t = 0	r = 2 t = 0
PD22	52	M	R	23	33	1- 165 Hz 4V 60 μ s	r = 2 t = 2	r = 1 t = 1	r = 2 t = 2
PD23	66	M	L	29	47	1-2+, 180 Hz 4V 60 μ s	r = 2 t = 0	r = 0 t = 0	r = 1 t = 0

Abbreviations: F= female; M=male; R=right; L=left; r= rigidity; t = tremor; na= not available